24th INTERNATIONAL CONGRESS ON SOUND AND VIBRATION
23–27 July 2017, London

ICSV24
23-27JULY 2017
LONDON CALLING

METASTRUCTURES FOR NOISE AND VIBRATION CONTROL

Keith Attenborough, Ho-Chul Shin, Shahram Taherzadeh

School of Engineering and Innovation, The Open University, Milton Keynes, UK
email: keith.attenborough@open.ac.uk

Logan Schwan[1], Olga Umnova

Acoustics Research Center, University of Salford, The Crescent, Salford, U.K.,

Abdelhalim Azbaid El Ouahabi, Victor Krylov

Department of Aeronautical and Automotive Engineering, Loughborough University, Loughborough, UK.

Metastructures, which include metamaterials and metasurfaces, can be designed to reduce noise and vibration at wavelengths considerably larger than their internal or topographical structure. Investigations are reported into reflection from arrays of resonant spheres at normal incidence, grazing incidence propagation over resonant structures on a hard surface and impedance matching to layers of absorbing materials using arrays of cylinders. Tube-in-sphere resonators are found to introduce a low frequency peak in the insertion loss at normal incidence and an extra ground effect dip at oblique incidence. Slits in hollow cylindrical and rectangular roughness elements increase attenuation due to ground effect. A gradient index sonic crystal array of cylinders provides impedance matching to a fibreglass layer and thereby broadband improvement in sound absorption. One or two rows of regularly-spaced parallel cylinders in front of porous sound absorbing layer are predicted also to improve absorption. Reduced scale ultrasonic transmission measurements comparing the efficacy of three surface treatments, (regular arrays of holes, random roughness and periodically-spaced grooves), for attenuating Rayleigh waves have found the regularly-spaced grooves to be the most effective.
Keywords: periodic, roughness, resonance, scattering, attenuation

1. Introduction

Multiple scattering by regular 2D arrays of solid cylinders in air at wavelengths comparable to the cylinder radius and spacing gives rise to reduced transmission at some frequencies (stop bands) and enhanced transmission (or focussing) at other frequencies (pass bands) depending upon the centre-to-centre spacing of the cylinders (the lattice constant). The amplitudes of the stop and pass bands depend on the fraction of the total volume of the array occupied by scatterers, known as the filling fraction, which depends on the lattice constant and the cylinder radius. Below the first stop band frequency, cylinders arrays may be modelled as effective fluids in which the effective sound speed depends on the filling fraction. A common method of improving the insertion loss provided by cylinder arrays is to employ locally resonant elements.

Ground surface roughness at heights less than the incident wavelengths modifies the reflection of sound. If direct and ground-reflected sound paths are sufficiently coherent they interfere constructively and destructively. Outdoors the result is known as ground effect. Roughness on acoustically-hard surfaces reduces the frequencies at which destructive interference occurs and can be used as a

[1] Now at LAUM, Université du Maine, France

method of controlling surface transport noise [1]. Arrays of locally resonant roughness elements, so-called 'metasurfaces', can be used to enhance low frequency attenuation due to ground effect. Investigations are reported involving arrays of spherical, cylindrical and rectangular resonators. In addition the use of cylinder arrays to provide impedance matching and thereby enhance the performance of sound absorbing layers is discussed and reduced scale investigations of surface treatment methods for attenuating Rayleigh seismic waves are reported.

2. Reflection from periodic resonant rough surfaces

2.1 Normal incidence

Surfaces with periodic profiles such as diffusers or air-backed microperforated panels are used widely for modifying room acoustics but, at frequencies below 300 Hz for example, would be required to be too large to be useful. On the other hand, a resonant rough 'metasurface' is capable of either total sound absorption or pressure-release reflection for incident wavelengths much larger than the corrugation height and spacing [2]. A tube-in-sphere resonator can be designed to have a resonant frequency far lower than would correspond to a hollow intact sphere of the same size [3]. A cut away schematic of a tube-in-sphere resonator design is shown in Fig. 1(a).

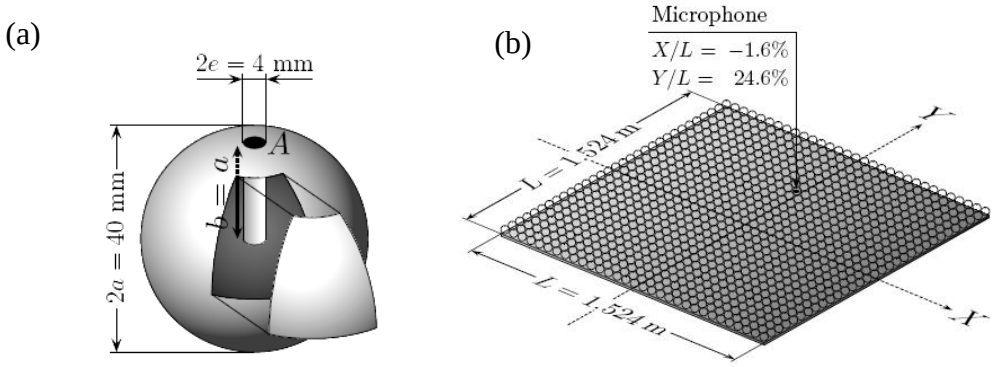

Figure 1: Schematics (a) of the design of a tube-in-sphere resonator and (b) of a 31× 31 square array of spherical resonators on a base and an example microphone location.

The resonant frequency, f_0, of a single tube-in-sphere resonator is given by $(1/2\pi)\sqrt{(K_0/M_0)}$ where $K_0 = (\pi e^2)^2\gamma P_{air}/V$, $V = (4/3)\pi a^3 - \pi e^2 b$, $M_0 = \rho_{air}\pi e^2 b$. P_{air} and ρ_{air} are equilibrium pressure and density in air. For the dimensions shown in Fig. 1(a), the resonant frequency is 237 Hz corresponding to a wavelength of 36 times the resonator diameter.

A 'metasurface' consisting of a 31× 31 square array of 4 cm diameter tube-in-sphere resonators (centre-to-centre spacing (L) 0.05 m) is represented in Fig. 1(b). According to homogenisation theory [2], a long-wavelength approximation for the normalised effective surface impedance of such an array, Z, obtained by using is given by

$$Z = \frac{1}{\eta}\left[2\zeta - i\left(\frac{f}{f_0} - \frac{f_0}{f}\right)\right]. \quad (1)$$

where $\eta = \frac{2\pi|A|^2 f_0}{K_0 \Sigma}$, $A = \pi e^2$, Σ is the periodicity (the unit cell area i.e. L^2 for a square array) and the damping factor ζ is determined from impedance tube data. Use of the normalised impedance given by Eq. (1) in the standard expression for the plane wave reflection coefficient at angle θ leads to a prediction of zero reflection (total absorption of plane waves) when $cos\theta = \eta/2\zeta \leq 1$.

Figure 2 compares measured and predicted insertion loss (IL) spectra, defined as the difference in spectral levels at a microphone 5 cm above the centre of the array base due to a loudspeaker source 2 m above the centre of the base measured without and with tube-in-sphere resonators) at normal incidence with different sizes of arrays (15×15 and 31×31). Measurements and predictions agree fairly well but, while the predicted frequency of the peak IL is the same for both arrays, the

measured peak frequencies are 257 Hz for the 15×15 array and 250 Hz for the 31×31 array. This may result from non-uniformity of the resonators. Average dimensions from a sample of 50 resonators were tube width and length 0.0046 m and 0.046 m respectively and an average outer diameter of 0.038 m. These average dimensions correspond to a resonant frequency of 275 Hz.

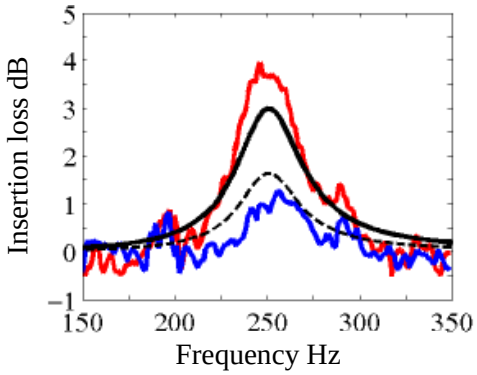

Figure 2: Measured (solid blue and red lines) and predicted (broken and solid black lines) insertion loss spectra due to 15×15 and 31×31 square arrays of tube-in-sphere resonators respectively.

2.2 Ground effect enhancement

2.2.1 Tube-in-sphere resonators

Measurements in an anechoic chamber have been made with a point source corresponding to the end of a tube fitted on a Tannoy loudspeaker at a height of 11 cm and a microphone at a height of 1 cm in the centre of arrays of intact spheres and tube-in-sphere resonators, 80 cm from the source. Figures 3(a) and (b) compare insertion loss (IL) spectra measured with a 15×15 array of intact spheres and 15×15 and 31×31 arrays of tube-in-sphere resonators. As well as introducing a low frequency destructive interference between 250 and 300 Hz corresponding to their resonant frequency (Fig. 3(a)), the tube-in-sphere resonators introduce roughness-related destructive interferences (see Fig. 3(b)). Above 1 kHz, the measured IL spectra for 15×15 arrays of intact (original) and resonant spheres are similar indicating that they are determined by roughness topography alone. The Tannoy point source used for these measurements was less powerful below 300 Hz than that (a B&K type 4295 loudspeaker) used at normal incidence (Fig. 2).

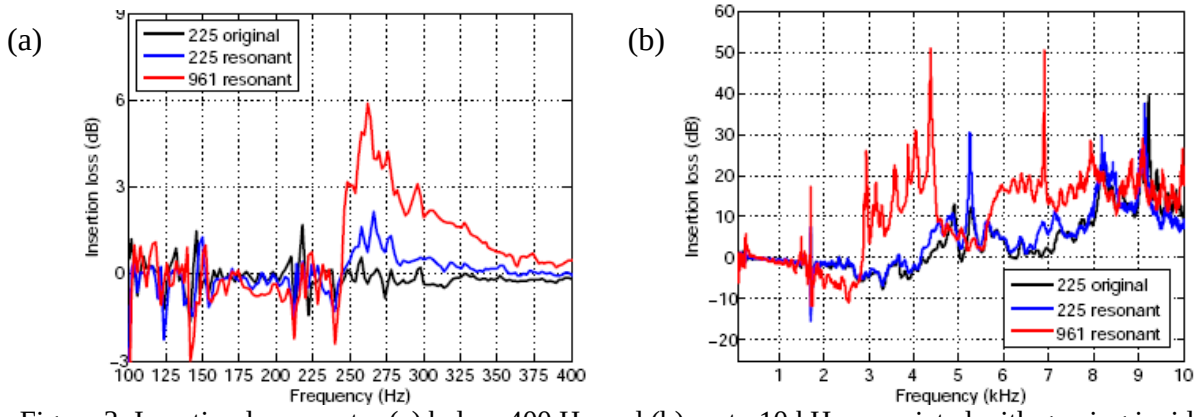

Figure 3: Insertion loss spectra (a) below 400 Hz and (b) up to 10 kHz associated with grazing incidence over a 15×15 array of intact spheres and 15×15 and 31×31 arrays of tube-in-sphere resonators

Figures 4(a) and (b) show data obtained for the differences in spectral levels measured at a microphone located 1.1 m from the B&K type 4295 point source loudspeaker at grazing angles of 0° and 32.6° over a hard surface and above 24×24 square arrays (L = 0.05 m) of tube-in-sphere resonators with elevated source and receiver corresponding to grazing angles between 24° and 38°. Also shown in Figs. 4(a) and (b) are predictions for a point source over a smooth hard surface and over a

surface with an effective impedance given by Eq. (1) with f_0 = 251 Hz, $\eta = 0.061$ and ζ = 0.074. The additional low frequency destructive interference associated with resonance near 250 Hz is predicted also by the classical theory for a point source over a plane with the surface impedance given by Eq. (1). Agreement with data and predictions for a point source over the effective impedance plane is improved by assuming f_0 = 281 Hz (see Fig. 4(b)). Again this can be attributed to non-uniformity of the tube-in-sphere resonators.

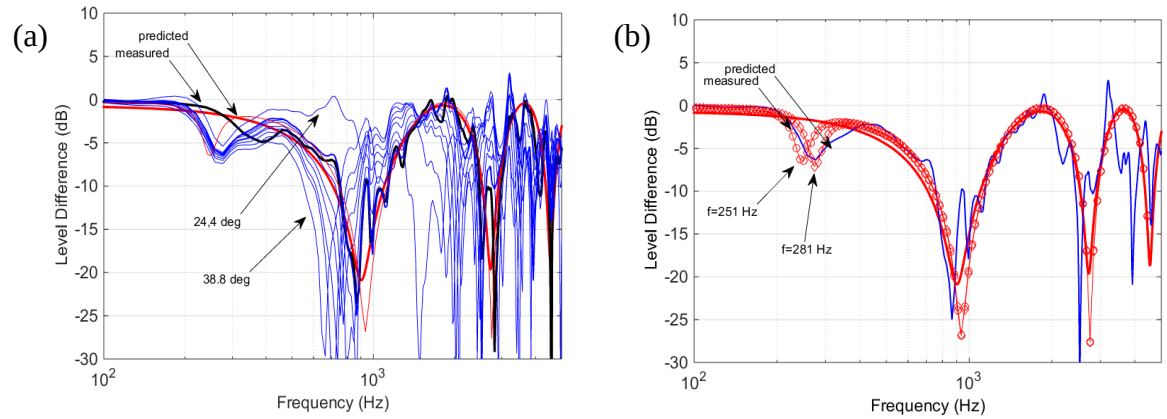

Figure 4: Thin solid blue lines are spectra of the difference in levels measured at grazing incidence 1.1 m from (point) source over a hard base and (a) measured at grazing angles between 24° and 38° over 31×31 square arrays tube-in-sphere resonators): (b) measured at grazing angle of 32.6° over a 24×24 array of tube-in-sphere resonators (L = 0.05 m). Joined symbols are level difference spectra predicted for a point source over a plane with impedance given by Eq. (1). The continuous black line in (a) represents the measured level difference spectra over the smooth base between grazing angles of 0° and 32.6°. The thick solid red lines are predicted level difference spectra over a smooth hard surface between grazing angles of 0° and 32.6°.

2.2.2 *Resonant cylinders and rectangles*

Enhancement of the ground effect due to other resonant roughness elements has been observed in laboratory measurements with (point) source height 0.08 m, receiver height 0.059 m separated horizontally by 0.95 m. Spectra of insertion loss (with respect to a smooth hard base) due to 9 cylinders (hollow PVC pipes with external and internal diameters of 0.055 m and 0.0526 m respectively) spaced regularly at 0.1 m apart, intact or each having a line of 0.3 m long 0.00263 m wide slits, are shown in Figs. 5(a) and (b) respectively.

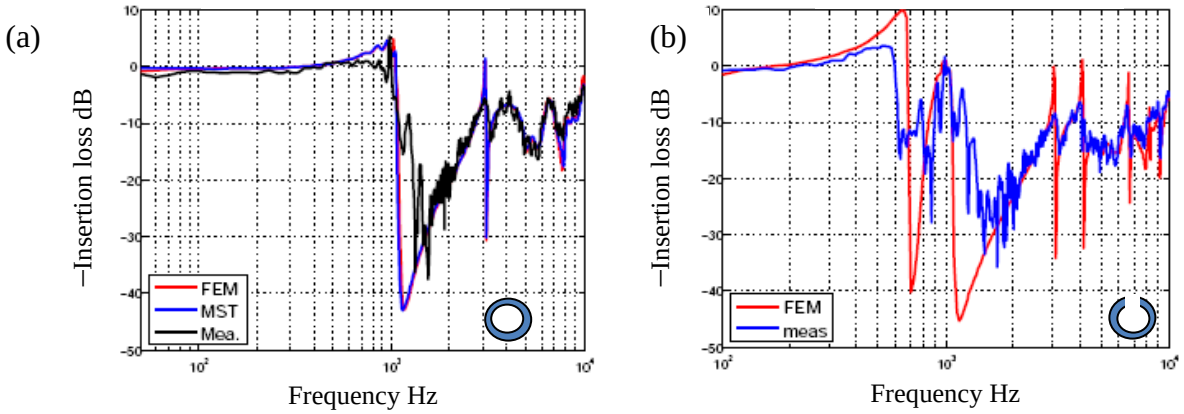

Figure 5: (Negative) Insertion loss spectra measured with (point) source height 0.08 m, receiver height 0.059 m separated horizontally by 0.95 m with 9 cylinders (OD 0.0526 m) (a) without (solid black line) and (b) with a series of 0.3 m long 0.00263 m wide slits (solid blue line). Also shown are predictions using Multiple Scattering Theory (MST) (solid blue line in (a)) and the Finite Element Method (FEM) (solid red lines in (a) and (b)).

The measured insertion loss spectrum over the intact cylinders is predicted by using either multiple scattering theory (MST) [4] or the Finite Element Method (FEM). FEM also gives predictions in

reasonable accordance with measurements for propagation over slit cylinders showing a destructive interference near 700 Hz in addition to that near 1.2 kHz associated with the effective impedance induced by the roughness topography above 1 kHz.

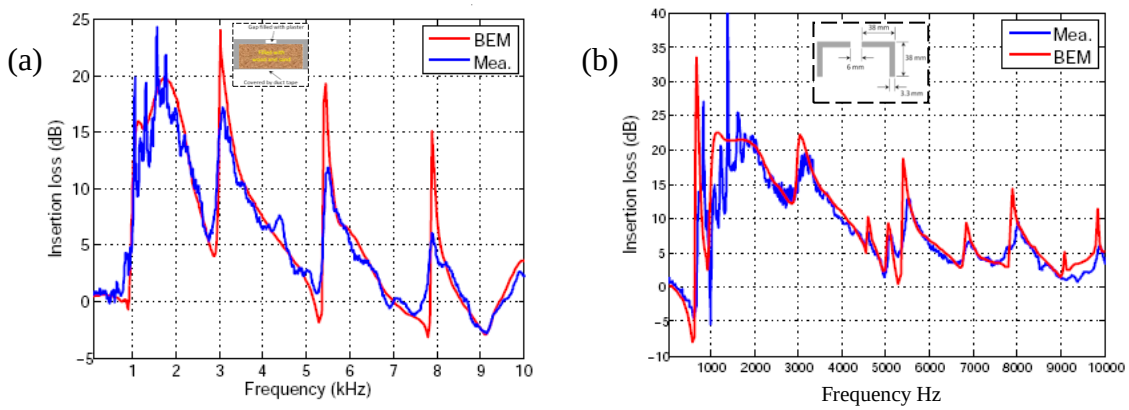

Figure 6: BEM-predicted (continuous red lines) and measured (continuous blue lines) insertion loss spectra between a point source at 0.08 m height and a 0.059 m high receiver separated horizontally by 0.95 m due to (a) an array of six 0.082 m wide 0.038 m high 'filled' pairs of aluminium angles (see inset) edge-to-edge spacing 0.15 m and (b) the same aluminium angle pairs with 0.006 m wide gaps (see inset).

Similar measurements and Boundary Element Method (BEM) predictions have been made over rectangular roughness elements constructed from aluminium angles [5]. Figure 6 shows measured insertion loss spectra (a) with six 0.082 m wide 0.038 m high rectangular strips formed from aluminium angle pairs filled with wood sand and plaster (see inset) and (b) the same strip constructions with 0.006 m wide gaps between the aluminium angles (i.e. before they were filled). The gaps result in an extra peak in the insertion loss below 1 kHz. Measurements have been made also with 'doubly-resonant' rectangular structures formed from two pairs of aluminium angles (see inset in Figure 7(a)). These compound structures result in additional peaks in the insertion loss. Practical constraints prevented the creation of the planned uniform 0.001 m wide inner gaps which should have been more effective than measured according to BEM simulations [5]. Nevertheless, as indicated by Figure 7(b) which shows an expanded plot of the measured spectra below 2 kHz in more detail, the doubly-resonant structure results in a larger overall insertion loss.

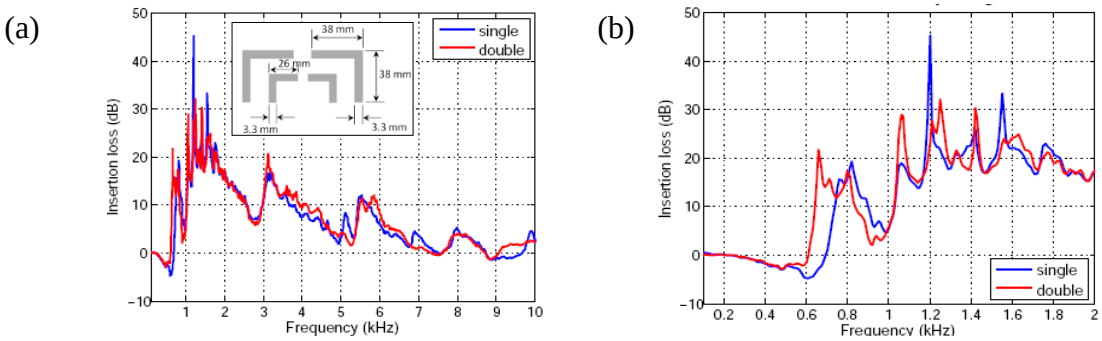

Figure 7: (a) Insertion loss spectra measured with point source at 0.08 m height and 0.059 m high receiver separated horizontally by 0.95 m due to 6 doubly-resonant rectangular structures each formed from 2 pairs of aluminium angles (see inset)) with edge-to-edge spacing of 0.15 m
(b) expanded plot of measured spectra below 2 kHz.

3. Sonic crystal assisted absorbers

At wavelengths large compared with the period of a regular array of rigid scatterers, the array may be considered to have an effective density and sound speed given by

$$\rho_{eff} = \frac{\rho_{air}(1+F)}{1-F}, \; c_{eff} = \frac{c_{air}}{\sqrt{1+F}}, \quad F < 0.6 \tag{2}$$

where c_{air} is the (adiabatic) sound speed in air and F is the filling fraction [6].

For a square array of cylinders of radius a with lattice constant l, $F = \pi a^2/l^2$. A gradient index sonic crystal (GRINSC) formed from regularly-spaced parallel cylinders with radii that gradually increase from the source side towards the surface of a hard-backed layer of absorbing material can be used to provide impedance matching from air to the material (see Figs. 8(a) and (b)).

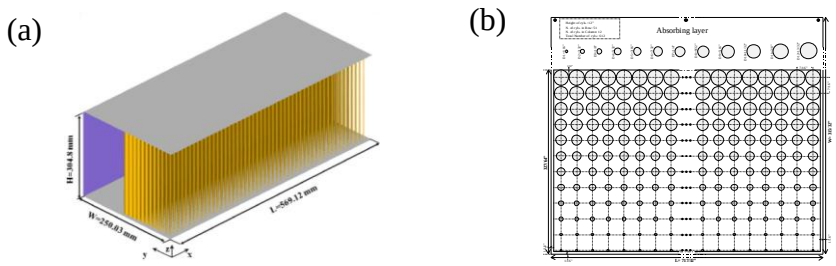

Figure 8. (a) Schematic of a sonic crystal assisted hard-backed absorbing layer in a box (b) cross section of a 12 row graded index array of cylinders.

Figure 9(a) compares the magnitudes of the pressure reflection coefficients deduced from measurements using a two microphone transfer function method with a loudspeaker source at 2 m from the surface of a 569 mm wide x 305 mm high x 120 mm thick slab of fibreglass alone (solid black line) and with an array of ten rows of 305 mm long brass cylinders spaced at 11 mm with radii increasing from 0.8 mm to 4.4 mm in steps of 0.4 mm (solid blue line) [7]. This GRINSC delivers a broadband increase in the absorption of the layer between 500 Hz and 3 kHz. Figure 9(b) shows predictions using Eqs. (2) and the transmission line formula for a two- or three-layer impedance including a final hard-backed 120 mm thick parallel slit layer (flow resistivity 50 kPa s m^{-2}, porosity 0.85) [8]. The predictions indicate that a row of 15 mm radius cylinders, with centre-to-centre spacing 60 mm, 30 mm in front of the slit layer gives a useful broadband reduction in reflection coefficient and that a large reduction near 500 Hz could be obtained using two rows; (1) l = 30 mm, a = 8 mm (F = 0.223, 40 mm wide) and (2) l = 50 mm, a = 20 mm (F = 0.503, 60 mm wide).

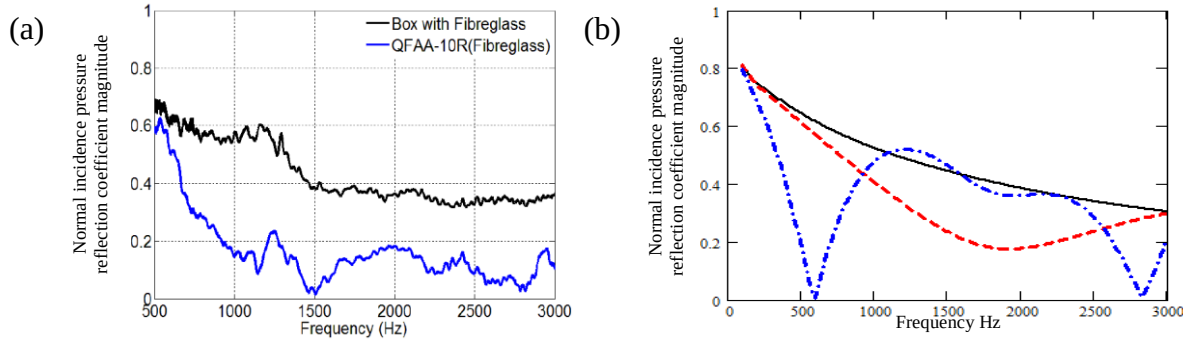

Figure 9: Pressure reflection coefficient magnitudes at normal incidence (a) measured with a 0.12 m thick layer of fibreglass only (black solid line) and after adding a 10 row graded index array of cylinders (blue solid line) (b) predicted for a hard-backed 0.12 m thick parallel slit absorber alone (solid black line), after adding a single row SC (red broken line: F = 0.196) and after adding a 2 row SC (blue dash-dot line: F = 0.223 and 0.503).

4. Rayleigh wave reduction

A series of measurements of 1 MHz ultrasonic pulse transmission have been carried out on 350 mm × 250 mm × 20 mm thick aluminium blocks (Rayleigh wave speed 2920 m/s) to investigate three methods of attenuating seismic Rayleigh waves. The first method involves drilling a periodic array of vertical holes and represents a reduced scale version of experiments carried out with seismic waves [9]. The second method creates random surface roughness and the third method introduces regularly spaced grooves. An example experimental arrangement is depicted in Fig. 10(a).

The distance, *D*, between source and receiver was 5 cm for measurements involving holes and grooves and 12 cm for measurements with random roughness. Figure 10(b) shows a square array of holes with diameter 1.2 mm, depth 9.2 mm and centre-to-centre spacing 3.2 mm. Figure 10(c) shows indentations produced by a hammer point and Fig. 10 (d) shows an array of six 29.4 mm long, 1.5 mm wide, 0.85 mm deep grooves with centre-to-centre spacing 2.9 mm.

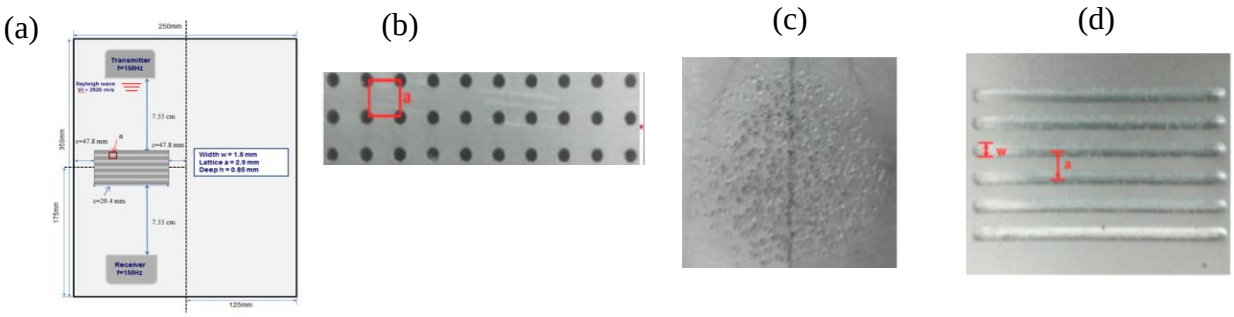

Figure 10: (a) An example arrangement of source, receiver and treated area (b) square array of holes (c) randomly rough area made with hammer points and (d) grooves.

Figures 11(a) and (b) compare examples of the rectified pulse spectra measured with a smooth surface and a surface containing a square array of holes (see Fig. 10(b)). Figures 12(a) and (b) show time domain plots from measurements over a smooth surface and a surface containing 6 regularly-spaced grooves (see Fig. 10(b)). The effectiveness of different surface treatments has been compared using an amplitude reduction factor defined as the ratio of the peak pulse amplitude measured for the treated surface to the peak amplitude measured for the smooth surface. Hole arrays with larger filling fractions were found to yield higher and less angle dependent attenuations. Amplitude reduction factors obtained for the treatments shown in Figs. 10(b) - (d) at normal incidence are compared in Table 1. The parallel grooves prove more effective than the other methods, however the hammer point indentations are comparatively shallow.

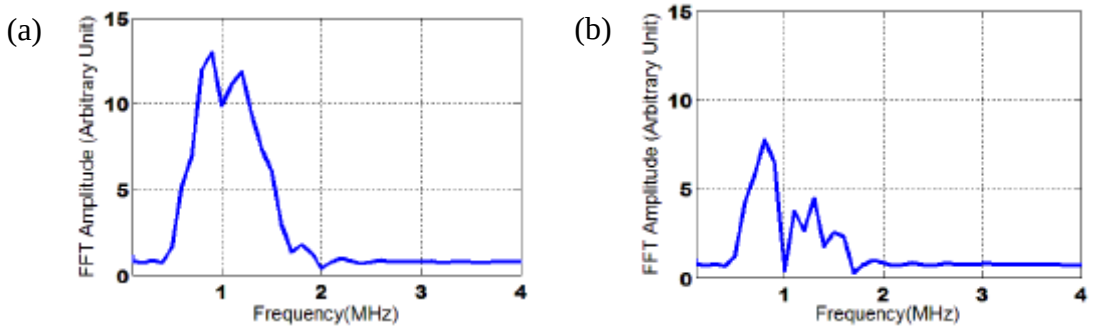

Figure 11: Spectra of rectified 1 MHz Rayleigh wave pulses measured on an aluminium block using the transmission arrangement shown in Fig. 10(a) with (a) a smooth surface and (b) a surface containing a square array of vertical holes (see Fig. 10(b))

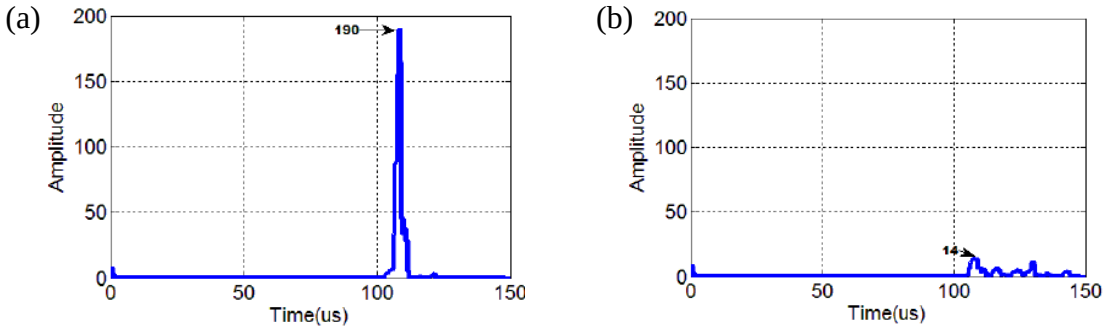

Figure 12: Time domain plots corresponding to measurements of rectified Rayleigh wave pulses on an aluminium block with source and receiver separated by 5 cm (a) on a smooth surface and (b) on a surface containing 6 regularly-spaced grooves (see Fig. 10(d))

Table 1: Amplitude reduction factors measured at normal incidence for three treatments (see Fig. 9)

Surface treatment	Square array of holes	Hammer point roughness	6 grooves
Amplitude reduction factor	0.36	0.73	0.04

5. Concluding remarks

Measurements and predictions show that tube-in-sphere resonator arrays provide low frequency absorption at normal incidence. The long wavelength theory given by Eq. (1) has been shown to agree with predictions of a multiple scattering theory yet to be published. These and other types of resonant roughness arrays on otherwise acoustically-hard surfaces contribute additional destructive interferences between direct and reflected paths for obliquely-incident sound at lower frequencies than those due to roughness topography alone. Absorption provided by layers of sound absorbing materials is increased by impedance matching using sonic crystal arrays of cylinders. Potentially cylinder arrays can be 'tuned' to achieve very high absorption at a target frequency. Ultrasonic measurements on an aluminium block have compared the efficacy of holes, surface roughness and grooves for attenuating Rayleigh waves and have shown that periodically-spaced grooves are most effective. Laser Doppler Vibrometer measurements on polymer foams (not reported here) have shown that mass loading of the surface also results in Rayleigh wave attenuation.

6. Acknowledgements

The authors are grateful to Peter Seabrook for help with the measurements at the Open University. The research has been supported by the U.K. Engineering and Physical Sciences Research Council (grant agreements EP/K037234/1, EP/K038214/1 and EP/K03720X/1).

REFERENCES

1 Taherzadeh, S., Bashir, I., Hill, T., Attenborough, K. and Hornikx, M., Reduction of surface transport noise by ground roughness, Applied Acoustics **83** 1-15 (2014).

2 Schwan, L., Umnova, O., Boutin, C., Shin, H-C., Taherzdeh, S. and Attenborough, K. Acoustic resonant surface: from nearly-total reflection to nearly-total absorption of sound, *Proceedings of EuroNoise 2015*, Maastricht, The Netherlands (2015).

3 Boutin, C., Acoustics of porous media with inner resonators, J. Acoust. Soc. Am. **134** 4717-4729 (2013).

4 Boulanger, P., Attenborough, K., Qin Q., and Linton C. M., Reflection of sound from random distributions of semi-cylinders on a hard plane: models and data, J. Phys. D. **38** 3480-3490 (2005).

5 Shin, H-C., Taherzadeh, S. and Attenborough, K., Ground effect due to periodic resonant roughness, *Proceedings of EuroNoise 2015*, Maastricht, The Netherlands (2015).

6 Torrent D., Håkansson, A., Cervera, F. and Sánchez-Dehesa, J., Homogenization of two-dimensional clusters of rigid rods in air, *Phys. Rev. Lett* 96, 204302 (2006).

7 Azbaid El Ouahabi, A. and Krylov, V.V., Experimental Investigations of Quasi-flat Acoustic Absorbers Enhanced by Metamaterial Layers, *Noise Theory and Practice*, December (2016). available: https://www.researchgate.net/publication/311984793

8 Attenborough, K., Li, K. M. and Horoshenkov, K. V. *Predicting outdoor sound*, Taylor and Francis, London and New York (2007).

9 Brûlé, S., Javelaud, E. H., Enoch, S. and Guenneau, S., Experiments on Seismic Metamaterials: Molding Surface Waves, Phs. Rev. Lett. 112, 133901 (2014)